

MONITORING SLOPE STABILITY DURING RAINFALL: A CASE STUDY USING SMALL-SCALE PHYSICAL MODELING

Gabriela Tuzzolo ¹; Rafael Ribeiro Plácido ²; Mariana Barbosa Juarez ³

¹ Scholarship Student of the GCSP – IMT (EEM/CEUN-IMT);

² Mentor of the GCSP-IMT (EEM/CEUN-IMT).

³ IMT Researcher (EEM/CEUN-IMT).

Article history: Received on 2024-11-08 / Presented at GCSP-IMT Seminar on 2024-12-05 /Available online from 2025-03-20

Abstract. *This study presents a GCSP research project focused on developing a small-scale physical model to analyze slope stability during rainfall. A steep soil slope (1:1) was built using samples from a landslide-prone area in Santos, SP. Tests under different simulated rainfall and load conditions exhibited failure mechanisms such as surface erosion and rotational landslides. Direct shear tests were conducted at water contents of 12% (optimum), 20% (unsaturated), and 30% (saturated). Cohesion values were 1 kPa, 20 kPa and 0 kPa, respectively, with friction angles ranging from 33° to 37°. Numerical modeling was used to calculate the safety factor, which increased under unsaturated conditions and decreased when the soil was assumed to be fully saturated. The experimental program also included calibrating a water content sensor for future monitoring applications. Research opportunities involve real-time predictive systems to reduce environmental and health risks.*

Keywords. *Slope Stability, Physical Modeling, Rainfall Simulator, Water Content Sensor, Risk Analysis.*

Introduction

In recent years, floods and landslides have been widely associated with global climate changes. The increase in atmospheric temperatures caused by human activities intensifies the hydrological cycle, leading to more intense and frequent rainfalls. Along with unplanned land use and population growth, these events raise the risk of landslides. The unregulated occupation of hillsides, often without proper drainage and infrastructure, compromises the safety and health of many people.

A clear example of the devastating impacts of this scenario is the tragedy that occurred on the northern coast of São Paulo State, Brazil, as shown in Figure 1. In February 2023, heavy rainfalls during the Carnival holiday caused landslides that led to hundreds of deaths and left thousands homeless (Globo, 2023). This event brought back memories of a similar disaster in 1967, when 436 people died due to landslides in the municipality of Caraguatatuba (Globo, 2017). These cases are not isolated. Coastal areas worldwide face similar tragedies year after year, especially in developing countries.

Landslides generally result from geotechnical instabilities, including shear strength reduction due to soil saturation and excess pore pressure during heavy rainfalls (Pinto, 2006). Additionally, poorly compacted soils, the lack of protective vegetation, and steep slope angles significantly contribute to landslides. The slope stability analysis involves calculating the safety factor, which is directly influenced by water content and saturation. Monitoring these critical parameters is essential for predicting failures and minimizing health and environmental risks.

Figure 1 – Landslide occurrence in February 2023 in Brazil (Globo, 2023)



Objectives

The main goal of this study is to conduct an experimental and computational program to analyze the impact of rainfall on slope stability and propose a preventive monitoring system to help prevent failures. The specific objectives include:

- To develop a small-scale physical model using soil samples collected from the city of Santos and a rainfall simulator, increasing soil saturation and applying loads (simulating building weight) until the formation of a failure surface.
- To determine Mohr-Coulomb failure envelopes through direct shear tests, considering the soil conditions before and after rainfall.
- Develop a numerical model to calculate the safety factor under unsaturated and saturated soil conditions to validate the physical model results and compare both cases.
- Calibrate a sensor to measure real-time water content and program it to emit preventive alerts when the safety factor reaches critical levels.

Development

- Soil characterization

The soil samples used in this research were collected from a hillside in Santos, a city located on the coast of São Paulo State. This study area was selected due to its rainfall patterns and geological-geotechnical profile, which contribute to high landslide susceptibility.

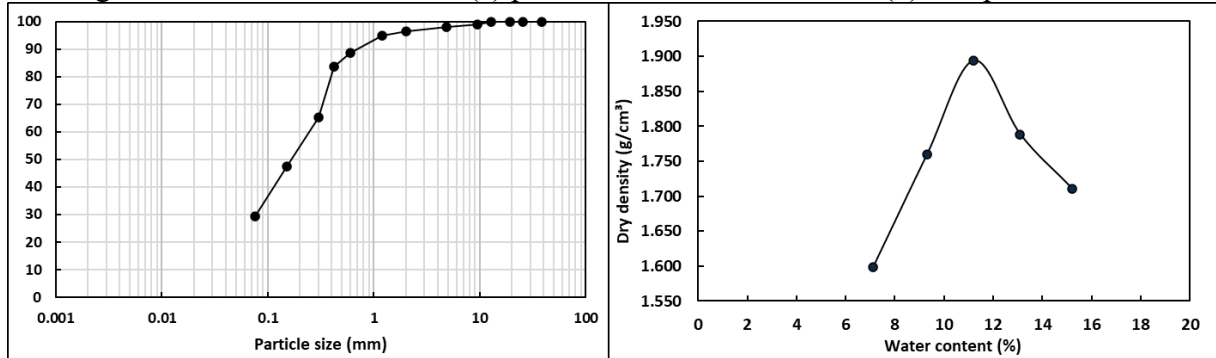
Particle size distribution consists of 3.6% gravel, 7.9% coarse sand, 32.1% medium sand, 27% fine sand, and 29.4% silt and clay (Figure 2a), classifying the soil as silty sand. Based on the compaction curve, the optimum moisture content is 12%, with a maximum dry density of approximately 1.9 g/cm^3 (Figure 2b). These parameters were essential for constructing the small-scale physical model, allowing soil compaction to replicate natural conditions and reflect slope behavior.

- Small-scale physical model

An acrylic box measuring 40 cm in length, 15 cm in width, and 30 cm in height was used for the small-scale physical model. It was sealed with silicone to prevent soil and water loss during tests. The soil slope was designed at a 1:1 ratio (45°), considered a critical stability condition for sandy soils, making it suitable for studying failure mechanisms.

The rain simulator was initially designed as a second acrylic box with small holes in its base, positioned above the first box. This upper compartment would be filled with water and simulate rainfall on the slope. However, during preliminary tests conducted using another soil, it was observed that even small-diameter holes caused excessive water impact. Each droplet behaved as a large particle, leading to intense surface erosion and compromising the small-scale model's integrity.

Figure 2 – Soil characteristics: (a) particle size distribution and (b) compaction curve

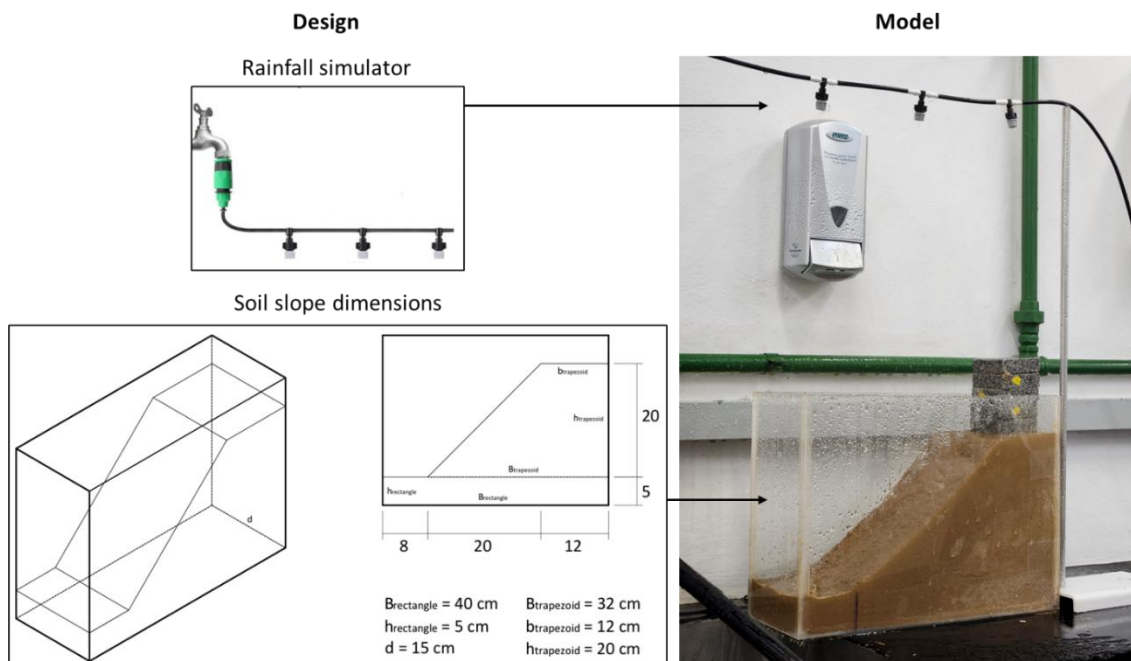


Then, the simulator was adjusted to reproduce the rainfall effect in a controlled manner. The adopted solution was to replace the second box with low-flow spray nozzles, similar to those employed in irrigation systems. These nozzles provided a more homogeneous, mist-like rainfall simulation, reducing droplet size and preventing excessive soil erosion.

Additionally, water that fell onto the model accumulated at the slope's toe, affecting soil saturation and failing to replicate the natural drainage process of a real-scale slope. To address this issue, a 1-cm hole was made at the base of the box, and a plastic tube was installed to allow controlled runoff of excess water.

Figure 3 illustrates both the design and construction of the small-scale physical model, including soil slope dimensions and the rainfall simulator.

Figure 3 – Desing and construction of the small-scale physical model



Two small-scale physical models (Model 1 and Model 2) were built using the soil from Santos. The material was prepared at water content of 12%, but it is worth mentioning that maximum compaction could not be achieved during placement into the box. Therefore, the total density (ρ) and dry density (ρ_d) of the soil were determined based on the total mass (M_{total}), total volume (V_{total}), and initial water content ($w_{initial}$), as shown in Equations 1 to 3:

$$V_{total} = [B_{rectangle} \times h_{rectangle} \times d] + \left[\left(\frac{B_{trapezoid} + b_{trapezoid}}{2} \right) \times h_{trapezoid} \times d \right] \quad (\text{Equation 1})$$

$$\rho = \frac{M_{total}}{V_{total}} \quad (\text{Equation 2})$$

$$\rho_d = \frac{\rho}{1 + w} \quad (\text{Equation 3})$$

Table 1 – Physical properties of the soil slope

Parameter	Value
Total mass of soil	17 kg
Total volume of soil	9,600 cm ³
Initial moisture content	12%
Total density	1.8 g/cm ³
Dry density	1.6 g/cm ³

Rock samples were placed at the top of the slope to simulate real-life loading conditions, such as the weight of houses and buildings. Both models were exposed to rainfall to study their behavior under increasing saturation and external load. At the end of tests, the water content was measured. Specimens using soil samples collected from the small-scale physical model were molded directly into the shear box to determine shear strength parameters.

c) Direct shear tests

Direct shear tests were performed in accordance with ASTM D3080/D3080M (2023) using a 10 cm x 10 cm square shear box. Previous consolidation was conducted under normal stresses of 100 kPa, 200 kPa, and 400 kPa for 24 hours. The horizontal displacement rate (R_d) of 0.16 mm/min was calculated using Equation 4, assuming a relative lateral displacement at failure (d_f) of 10 mm (10% of the specimen's length) and a minimum time to failure (t_f) of 60 minutes:

$$R_d = \frac{d_f}{t_f} \quad (\text{Equation 4})$$

Mohr-Coulomb failure envelopes were used to establish the soil's friction angle (ϕ) and cohesion (c). A total of three direct shear tests were conducted: the first at the optimum water content ($w = 12\%$), and the second and third at the water content measured after the completion of Model 1 and Model 2, respectively.

d) Numerical model

Numerical modeling was conducted using SLIDE2 by Rocscience for slope stability analysis and failure surface visualization. The input parameters included total unit weight (γ), saturated unit weight (γ_{sat}), c , and ϕ . Three distinct scenarios were modeled based on conditions observed during physical modeling and direct shear tests results. The software calculated the safety factor using the simplified Bishop method and displayed the potential failure surfaces for each scenario. Numerical and experimental data were compared to validate the study.

e) Water content sensor

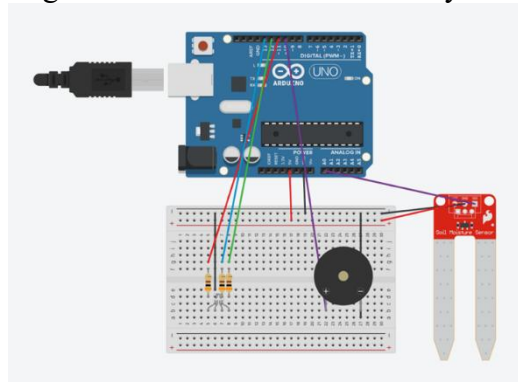
During the development of the monitoring system, a circuit was assembled using an Arduino Uno board, a water content sensor module, a buzzer, a 5-mm RGB LED, and three

300-ohm resistors. The sensor was designed to provide real-time readings of the water content. It operates based on changes in electrical resistivity, which varies as the water content changes.

The circuit was configured to detect water content levels and trigger specific responses. The Arduino code reads data from the sensor and controls the RGB LED and buzzer. The LED emits green for safe conditions, blue for intermediate caution, and red when the soil reaches a critical water content. In this emergency state, the buzzer signals the imminent risk of landslide.

This critical water content was determined through the experimental program described in the previous sections. Soil samples under varying water contents were used to calibrate the sensor. A calibration curve was created by plotting the sensor readings recorded for each sample against the actual water content. Figure 4 shows all system components.

Figure 4 – Water content sensor system



To provide a better understanding of the circuit's functionality, an online simulation was created using TinkerCAD software. The circuit and programming code can be viewed and tested in the following link: <https://www.tinkercad.com/things/gbvMRTzaCSG-sensor-umidade>.

Results and Discussion

a) Small-scale physical model

Figure 5 shows the failure mechanisms observed during rainfall simulations with Model 1 and Model 2.

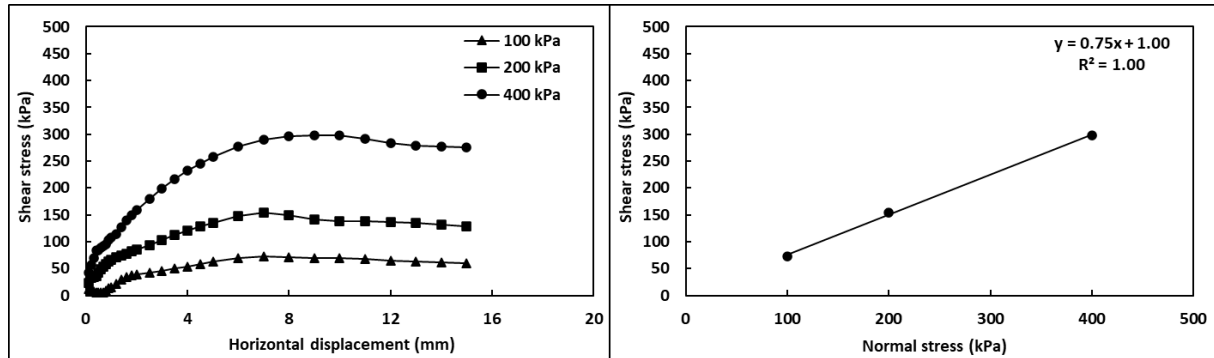
Figure 5 – Failure mechanisms of surface erosion (a) and rotational landslides (b)



b) Direct shear tests

The results of direct shear tests on soil samples prepared at the optimum water content of 12%, along with the corresponding Mohr-Coulomb failure envelope, are presented in Figure 6. The soil cohesion was 1 kPa, and the friction angle was 37°.

Figure 6 – Direct shear test on soil samples at the optimum water content



In Model 1, rotational landslides did not occur; instead, significant surface erosion was observed (Figure 5a), attributed to the height of the rainfall simulator. To better understand this behavior, direct shear tests were performed on samples collected from the model. As shown in Figure 7, c increased to 20 kPa, while ϕ slightly decreased to 33°. With water content near 20%, the soil was assumed to be unsaturated, and matric suction induced apparent cohesion (Carvalho et al., 2015).

In Model 2, the height of the rainfall simulator was adjusted to improve water infiltration into the soil and prevent surface erosion. This adjustment led to the occurrence of rotational landslides (Figure 5b). The water content measured at the end of the test was 30%. The results of subsequent direct shear tests support the hypothesis of matric suction, as cohesion was null under saturated conditions.

Figure 7 – Direct shear test on unsaturated and saturated soil samples

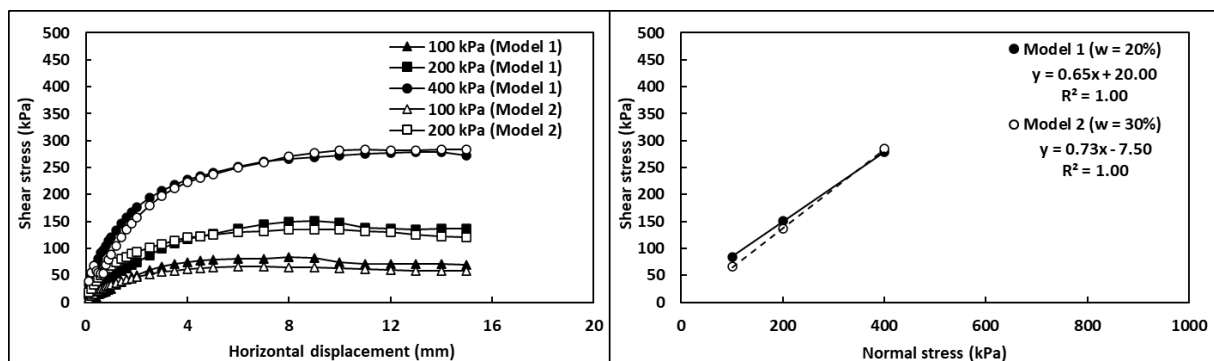
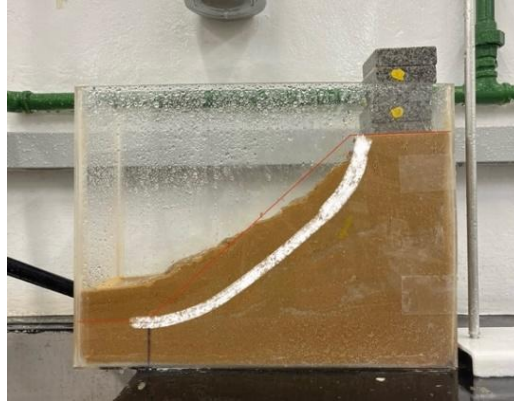


Figure 8 captures the landslide during the second test. The initial boundaries are marked in red, and the white line delineates the failure surface formed. This representation highlights the progression of mass movements and deformations under increased saturation.

Figure 8 – Estimated failure surface in Model 2



c) Numerical model

The first step in numerical modeling using SLIDE2 software was to adjust the scale of the model. Tests were conducted using scales of 1:100, 1:50, 1:20, and 1:10. The scale that best fits the analysis was 1:10 due to the reduced size of the physical model. Additionally, the load applied at the top of the slope, which corresponds to 1.35 kg in the small-scale physical model, produced unrealistically high values when converted to larger scale.

Three scenarios were modeled, each considering a distributed load of 25 kN/m² at the top of the slope and a total unit weight of 18 kN/m³. Table 2 summarizes the input parameters for each scenario. At the optimum water content (before rainfall), the calculated safety factor was 1.12, with the failure surface indicated in Figure 9. A higher safety factor (>1.50) was likely not reached due to the steepness of the slope.

Table 2 – Input parameters used to model the slope before and after rainfall

Scenario	1	2	3
Total unit weight	18 kN/m ³	18 kN/m ³	18 kN/m ³
Saturated unit weight	-	-	20 kN/m ³
Cohesion	1 kPa	20 kPa	0 kPa
Friction angle	37°	33°	35°
Water table	No	No	Yes

Figure 10 presents the results of the second (unsaturated) and third (saturated) scenarios, representing different post-rainfall conditions. Increasing cohesion from 1 to 20 kPa resulted in a safety factor was 3.17 (Figure 10a). It reflects the stability enhancement provided by matric suction. In the third scenario, where the soil was fully saturated and cohesion decreased to 0 kPa, the safety factor was significantly reduced to a critical value of 0.23. The resulting failure surface closely resembled that observed in the small-scale physical model (Figure 8), validating the methodology of this study and demonstrating a good correlation between the experimental and numerical data.

Figure 9 – Safety factor before rainfall

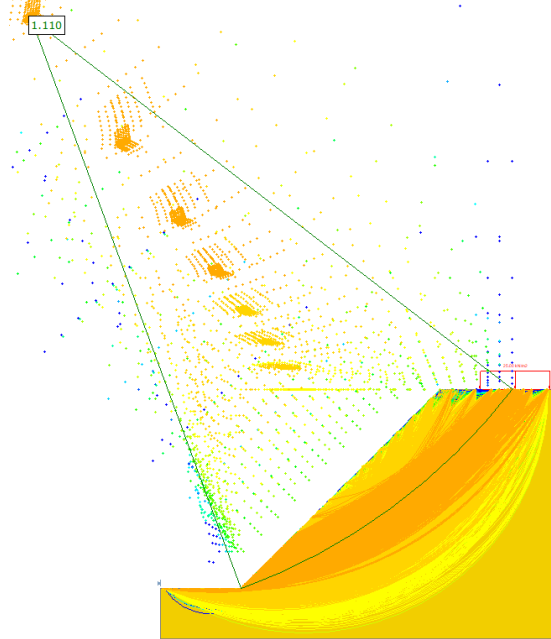
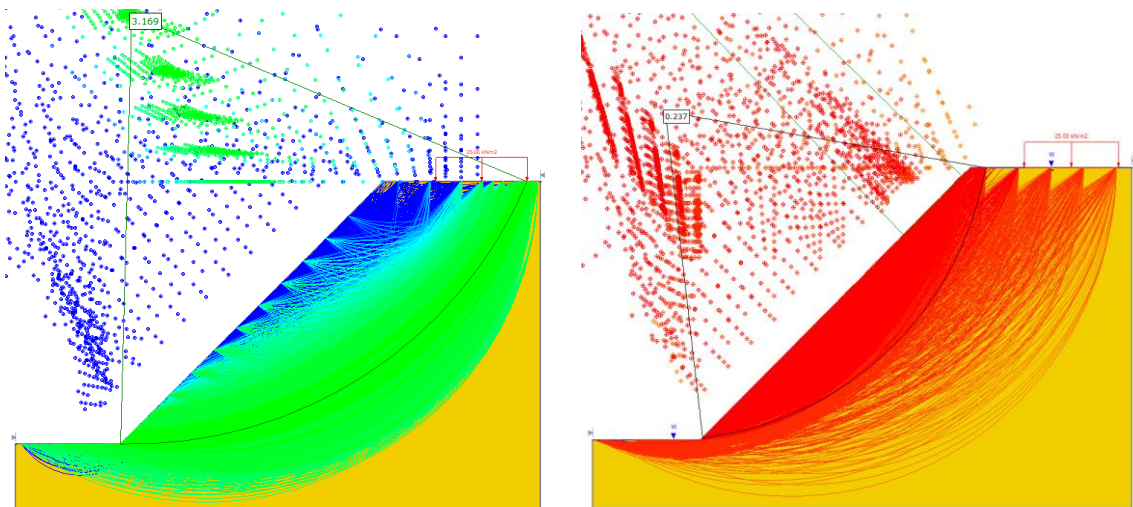


Figure 10 – Safety factor for unsaturated (a) and saturated (b) soil conditions



d) Sensor calibration

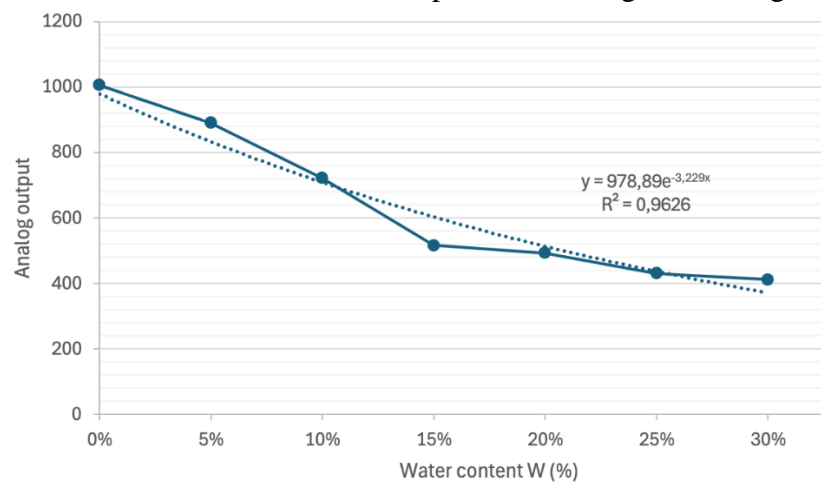
During calibration of the sensor, it was observed that when water content exceeded 30% (saturation degree of 100%), the Arduino's analog output remained nearly constant. This may occur because the sensor measures water in soil pores, and once fully saturated, additional water cannot infiltrate. The study conducted by Oliveira (2018) supports this hypothesis, showing that the sensor's response stabilizes at saturation, and its accuracy reduces.

Soil samples with water content ranging from 0% to 30% were prepared, and six readings were taken for each sample (0, 30, 60, 120, 180, and 300 s). Data are presented in Table 3, with exponential fitting applied given that resistivity-based sensors exhibit a non-linear behavior (Oliveira, 2018). The 0-second readings provided the best fit, with the coefficient of determination (R^2) of 0.96, as shown in Figure 11.

Table 3 – Coefficient of determination of exponential fitting for different readings

Reading	R ²
0s	0,9626
30s	0,9321
60s	0,9269
120s	0,9155
180s	0,9212
300s	0,9234

Figure 11 – Calibration curve and exponential fitting for reading at 0s



To validate the calibration, water content and analog sensor reading were recorded for soil samples collected from small-scale physical models. Table 4 shows the measured and estimated water content using calibration curve fitting. The results showed good agreement, confirming the sensor's effectiveness.

Table 4 – Estimative of water content using sensor

Sample	Measured water content	Sensor reading	Estimated water content
Optimum water content	12%	580	16.21%
Model 1	20%	470	22.72%
Model 2	30%	705	27.33%

Conclusion

This study assessed the effects of rainfall on slope stability by applying soil mechanics principles and constructing a small-scale physical model to investigate failure mechanisms. The research included a series of laboratory characterization tests, such as water content, physical properties, and direct shear tests. The matric suction contribution to shear strength highlighted the complexity of unsaturated soil behavior.

The results support the effectiveness of small-scale physical modeling to analyze soil slopes under increasing saturation. Numerical models in SLIDE2 software and their respective safety factors and failure surface showed good agreement with experimental data. Despite some limitations related to model scale and the use of a single soil type, this methodology provided

valuable insights into slope stability. The study also introduced an innovative approach using calibrated sensors able to monitor water content in real time, with potential applications in alert systems and geotechnical risk mitigation for landslide-prone areas.

Future research should address various soil types, slope angles, rainfall intensities, and loads. Improving the control and monitoring of these parameters during tests is recommended, along with the implementation of advanced numerical modeling techniques to incorporate their variation. Finally, the development of medium- and large-scale physical models could benefit from more robust sensors and geophysical methods.

References

ASTM 2023, D3080/D3080-M, Standard Test Method for Direct Shear Test of Soils Under Consolidated Drained Conditions.

Carvalho, JC, Gitirana Junior, GFN, Machado, SL, Mascarenha, MMA & Silva Filho, FC 2015, Solos não saturados no contexto geotécnico. São Paulo: Associação Brasileira de Mecânica dos Solos e Engenharia Geotécnica.

Globo 2017, Deslizamento de terra que devastou Caraguatatuba completa 50 anos, viewed 15 May 2024, <https://g1.globo.com/sp/vale-do-paraiba-regiao/noticia/2017/03/deslizamento-de-terra-que-devastou-caraguatatuba-completa-50-anos.html>

Globo 2023, Temporal devastador no Litoral Norte de SP completa uma semana: veja resumo da tragédia, viewed 15 May 2024, <https://g1.globo.com/sp/vale-do-paraiba-regiao/noticia/2023/02/26/temporal-devastador-no-litoral-norte-de-sp-completa-uma-semana-veja-resumo-da-tragedia.ghtml>

Oliveira, CL 2018, Calibração de sensores de umidade do solo de baixo custo, Monografia (Graduação em Agronomia), Universidade Federal Rural de Pernambuco, Garanhuns, Pernambuco, Brasil.

Pinto, CS 2006, Curso Básico de Mecânica dos Solos, 3. ed. São Paulo: Oficina de Textos.